An Optimal Control Approach for Communication and Motion Co-optimization in Realistic Fading Environments

Usman Ali,* Yuan Yan,** Yasamin Mostofi** and Yorai Wardi*

***Abstract*— We consider an energy co-optimization problem of minimizing the total communication and motion energy of a robot tasked with transmitting a given number of information bits while moving along a fixed path. The data is transmitted to a remote station over a fading channel, which changes along the trajectory of the robot. While a previous approach to the problem used a speed-based motion-energy model, this paper uses acceleration both as an input to the system and as a basis for the motion energy which is more realistic. Furthermore, while previous approaches posed the problem in discrete time, we formulate it in continuous time. This enables us to pose the problem in an optimal control framework amenable to the use of maximum principle. We then compute the optimal control input via an effective algorithm recently developed by us that converges very fast. We use practical models for channel fading and energy consumption: the channel quality is predicted based on actual measurements, and the energy models are based on physical principles. Simulation is used to solve a specific problem and demonstrate the efficacy of our proposed approach.**

I. INTRODUCTION

In the past several years, there has been a considerable interest in the area of mobile sensor networks and networked robotic systems [1]–[3]. More recently, communication-aware robotics has started to attract attention [4]–[6]. The underlying philosophy of communication-aware robotics is the fact that the motion of the robot impacts its connectivity and that communication disk models, which have commonly been used in the robotics literature, do not suffice to capture realistic connectivity issues for the purpose of path planning. Communication-aware robotics is then a multi-disciplinary approach to robotic path planning and decision making that properly co-optimizes the sensing, communication and navigation issues, while considering realistic link models.

The first important aspect of communication-aware robotics is the realistic modeling of communication links, beyond the over-simplified disk models. Along this line, Mostofi et. al [7] proposed a framework for probabilistic prediction of communication links in realistic fading environments, and showed how to successfully integrate it with robotic sensing and path planning [4], [5], [8]. This probabilistic approach has also started to be used in other navigation work [9]–[11].

*School of Electrical and Computer Engineering, Georgia Institute of Technology, Atlanta, GA 30332. Email: usmanali@gatech.edu, ywardi@ece.gatech.edu.

**Department of Electrical and Computer Engineering, University of California, Santa Barbara, CA 93106. Email: yuanyan@ece.ucsb.edu, ymostofi@ece.ucsb.edu.

Research supported in part by the NSF grant number CNS-1239225 and in part by the NSF grant number NeTS-1321171.

The second important aspect of communication-aware robotics is the co-optimization of both communication and motion energy usage. While individual optimization of communication and motion energy consumption has been heavily but separately explored in the communications/networking and robotics literature [12]–[14], co-optimization of communication and motion energy consumption has only started to attract attention recently. In [15], the authors designed an efficient algorithm to find the path that minimizes the motion and communication energy costs. In [16], the authors proposed algorithms to optimize the relay configuration in a data-intensive wireless sensor network, in order to minimize the total communication and motion energy costs of the sensors. In [17], the authors designed an algorithm to maximize the lifetime of the wireless sensor network, while considering both the communication and motion costs of the sensors. In [18], Jaleel, et. al proposed an optimal control approach to minimize the communication and motion energy costs in a one-dimensional robotic router network. However, simplified path-loss-only models are utilized to model the communication channels in the aforementioned papers. In [6], [19], Yan et. al proposed a co-optimization strategy that minimizes both communication and motion energy costs of the robot by properly co-optimizing the motion speed, transmission rate and stop times, under time constraint and in realistic fading communication environments.

In this paper, we consider the energy co-optimization scenario of [19]. More specifically, a mobile robot needs to transmit a fixed number of information bits to a remote station in a realistic fading communication environment, while moving along a given trajectory. Our goal is to minimize the total energy cost of the robot, including both communication and motion costs, while satisfying time budget and communication reception quality constraints. In [19], this problem is solved in a discrete fashion where a first-order dynamical model for the robot is assumed, without considering the acceleration cost. In practice, it is important to consider the acceleration cost. For instance, if the channel quality is improving, the robot may need to slow down to take advantage of the good connectivity for transmission (as shown in [19]). However, a realistic motion model that considers the acceleration cost may not allow the robot to slow down as fast as needed, impacting the whole transmission performance and energy consumption.

Thus, in this paper, we use a second-order motion model and a more complete motion cost that incorporates the acceleration while posing the whole setup in the continuous domain. This continuous time reformulation enables

us to pose the problem in an optimal control framework amenable to the use of maximum principle and compute the optimal control via an effective algorithm. Specifically, we use the Hamiltonian-based algorithm proposed in [18] which displayed fast and effective convergence for such optimal control problems [20]. This algorithm, summarized in the sequel, is especially suitable for continuous-time problems whose Hamiltonian has special properties. We demonstrate the efficacy of our algorithm by testing it on the considered problem and recording the CPU times required to compute the optimal control.

Our results show that the robot should transmit faster at the regions where the channel quality is better, as expected. However, we see new behaviors compared to the results in [19] where there are rapid changes in robot's velocity to changes in channel quality. In our case, because of the acceleration in the cost and as an input, the response of the velocity to the channel quality is more smooth and delayed. Again, due to the presence of acceleration in the cost, we see a smoother acceleration profile than would have resulted if we had ignored the acceleration as in [19].

The rest of the paper is organized as follows. Section II presents the previously-proposed probabilistic channel prediction framework of [7], [8] and formulates the optimal control problem. Section III describes the proposed algorithmic approach to it. Section IV presents simulation results and Section V concludes the paper.

II. Problem Formulation

In this section, we first present our probabilistic channel prediction framework that allows the robot to predict the channel quality at unvisited locations along the trajectory based on a small number of a priori Channel to Noise Ratio (CNR)[1] measurements in the same environment. Then, we show how the robot can assess its average communication energy cost, given a required receiver reception quality. Next we discuss the general motion cost model that incorporates the effects of acceleration. Finally, we pose the co-optimization problem in the optimal control framework.

A. Probabilistic Channel Prediction Framework [7], [8]

In the communication literature [12], it is well-known that the CNR can be modeled as a multi-scale random process with three components: path loss, shadowing and multipath fading. Thus, we can assess the channel quality probabilistically, at an unvisited location, based on only a small number of a priori channel measurements.

In [7], Mostofi, et. al showed that a Gaussian random variable, $\gamma_{\text{dB}}(q)$, can best characterize the CNR (in the dB domain) at an unvisited location q, where the mean and variance of $\gamma_{\text{dB}}(q)$ are given as follows:

$$\overline{\gamma}_{\text{dB}}(q) = H_q\mu + \Psi^{\text{T}}(q)\Phi^{-1}\big(Y - H_{\mathscr{Q}}\mu\big), \tag{1}$$

$$\Sigma(q) = \xi_{\text{dB}}^2 + \rho_{\text{dB}}^2 - \Psi^{\text{T}}(q)\Phi^{-1}\Psi(q). \tag{2}$$

[1]In this paper, CNR is defined as the channel power divided by the receiver noise power. Then, the received Signal to Noise Ratio will be CNR times the transmitted power.

Here, Y is the stacked vector of m a priori-gathered CNR measurements, $\mathscr{Q} = \{q_1, \cdots, q_m\}$ denotes the set of the measurement positions, $H_q = [1 \; -10\log_{10}(\|q - q_b\|)]$, $H_{\mathscr{Q}} = [\mathbf{1}_m \; -D_{\mathscr{Q}}]$, $\mathbf{1}_m$ represents the m-dimensional vector of all ones and q_b is the position of the remote station. Furthermore, $D_{\mathscr{Q}} = \big[10\log_{10}(\|q_1 - q_b\|) \cdots 10\log_{10}(\|q_m - q_b\|)\big]^{\text{T}}$, $\Phi = \Omega + \rho_{\text{dB}}^2 I_m$ with Ω denoting a matrix with entries $\big[\Omega\big]_{i,j} = \xi_{\text{dB}}^2 \exp(-\|q_i - q_j\|/\beta)$, for $i, j \in \{1, \cdots, m\}$, and $\Psi(q) = \big[\xi_{\text{dB}}^2 \exp(-\|q - q_1\|/\beta) \cdots \xi_{\text{dB}}^2 \exp(-\|q - q_m\|/\beta)\big]^{\text{T}}$. Finally, $\mu = [\alpha \; n_{\text{PL}}]^{\text{T}}$, ξ_{dB}, β and ρ_{dB} represent the channel parameters. Essentially, this channel prediction framework models the wireless channel as a non-stationary Gaussian random process. Then, the CNR at an unvisited location can be predicted by conditioning on the available a priori measurements in the same environment. See [7], [8] for more details on how the underlying parameters are estimated and the performance of this framework with real data and in different environments.

B. Communication Energy Model

Assuming the commonly used MQAM modulation for the communication from the robot to the remote station, the required transmit power at time t can be found as follows [12]: $\widetilde{P}_{\text{comm}}(t) = (2^{R(t)} - 1)/(K\Upsilon(q(t)))$, where $K = -1.5/\ln(5p_{b,\text{th}})$, $p_{b,\text{th}}$ is the given required Bit Error Rate (BER) threshold (i.e. the required reception quality), $R(t)$ denotes the spectral efficiency at time t, $q(t)$ is the position of the robot at time t, and $\Upsilon(q(t))$ represents the instantaneous CNR at $q(t)$.

As discussed in Section II-A, the CNR at unvisited location $q(t)$ is unknown but can be predicted as a lognormal random variable with its mean and variance given by (1) and (2) respectively. As a result, the anticipated communication power is also random. We then have the following for $P_{\text{comm}}(t)$, the average communication power (averaged over the predicted channel), which we use in the rest of the paper:

$$P_{\text{comm}}(t) = \frac{2^{R(t)} - 1}{K} E\left[\frac{1}{\gamma(q(t))}\right]. \tag{3}$$

Note that for lognormally distributed $\gamma(q(t))$, we have

$$E\left[\frac{1}{\gamma(q(t))}\right] = \exp\left(\left(\frac{\ln 10}{10}\right)^2 \frac{\Sigma(q(t))}{2}\right) \frac{1}{\overline{\gamma}(q(t))}, \tag{4}$$

where $\overline{\gamma}(q(t)) = 10^{\overline{\gamma}_{\text{dB}}(q(t))/10}$. As can be seen, equation (4) is a measure of the predicted channel quality at $q(t)$. In this paper, we say the predicted channel quality is high (low) if (4) is small (large).

C. Motion Energy Model

Suppose that the robot is moving with a velocity $v(t)$ and an acceleration $u(t)$ along the pre-defined trajectory due to an applied force generated by the DC motor of the robot. Without loss of generality, $v(t)$ and $u(t)$ are scalars, since we only need to consider the magnitude and direction of

the acceleration and velocity along the trajectory. Then the motion power consumed in the process is given by [13]

$$P_{\text{mo}}(t) = k_1 u(t)^2 + k_2 v(t)^2 + k_3 v(t) + k_4 + k_5 u(t) + k_6 u(t) v(t), \tag{5}$$

where k_i, $i \in \{1, \cdots, 6\}$, is a constant. Note that (5) includes the impact of both velocity and acceleration. Also, the motion model used in [19] is a special case of (5) when k_1, k_5 and k_6 are equal to 0.

D. Optimal Control Problem

Consider a second-order dynamic model for the motion of robot as follows: $\dot{x} = v(t)$ and $\ddot{x}(t) = u(t)$. We define the state variables as $x_1 = x$ and $x_2 = \dot{x}$ and take the acceleration $u(t)$ as the control variable. We get the following state equations:

$$\begin{aligned} \dot{x_1}(t) &= x_2(t), \\ \dot{x_2}(t) &= u(t). \end{aligned}$$

Note that x_1 is a scalar which represents the total distance traveled along the pre-defined trajectory. The force $F(t)$ required to produce this acceleration $u(t)$ is $F(t) = Mu(t) + g(x_1(t), x_2(t))$ where $g(x_1(t), x_2(t))$ is the force incorporating the effects of air drag, friction and gravity along the path of travel, and M is the mass of the robot.

We then have the following continuous-time formulation of the co-optimization problem:

$$\begin{aligned} \text{minimize} \quad & J_1 = \int_0^{t_f} \left(\frac{2^{R(t)} - 1}{K} s(x_1(t)) + k_1 u(t)^2 + k_2 x_2(t)^2 \right. \\ & \left. + k_3 x_2(t) + k_4 + k_5 u(t) + k_6 u(t) x_2(t) \right) dt \\ \text{subject to} \quad & \dot{x}_1(t) = x_2(t), \qquad x_1(0) = a, \quad x_1(t_f) = b, \\ & \dot{x}_2(t) = u(t), \qquad x_2(0) = 0, \quad x_2(t_f) = d, \\ & \int_0^{t_f} R(t) dt = \frac{Q}{B}, \quad -u_{\max} \le u(t) \le u_{\max}, \\ & 0 \le R(t) \le R_{\max}, \end{aligned} \tag{6}$$

where the control input consists of acceleration $u(t)$ and spectral efficiency $R(t)$, for $t \in [0, t_f]$, t_f is the total time budget, $s(x_1(t)) = E\left[\frac{1}{\gamma(q(x_1(t)))}\right]$ with $q(x_1(t))$ denoting the mapping from $x_1(t)$ to the corresponding position along the pre-defined trajectory, $u_{\max}$ and $R_{\max}$ denote the maximum achievable acceleration and spectral efficiency respectively, Q is the total number of information bits to be sent and B is the given communication bandwidth. Since the robot travels along a fixed trajectory, we consider the case where the robot starts from position a and needs to move to position b at the end of operation. Moreover, we assume that the robot is stationary initially, i.e. $x_2(0) = 0$, and needs to reach velocity d at time t_f. Note that constraint $\int_0^{t_f} R(t) dt = Q/B$ guarantees that the information bits are sent to the remote station within the given time budget.

To pose the integral constraint in (6) in a way amenable to compute the optimal control, we define the auxiliary state variable x_3 in the following way:

$$\dot{x}_3 = R, \qquad x_3(0) = 0, \quad x_3(t_f) = \frac{Q}{B} := c. \tag{7}$$

The problem now becomes that of minimizing J_1 defined in (6) subject to the dynamic constraints defined via (6) and (7), as well as pointwise input constraints of the form $|u(t)| \le u_{\max}$ and $0 \le R(t) \le R_{\max}$. We handle the terminal constraints in (6) and (7) by using penalty functions comprised of quadratic terms. Hence, for constants $C_1 \ge 0$, $C_2 \ge 0$, and $C_3 \ge 0$, the optimal control problem has the form:

$$\begin{aligned} \text{minimize} \quad & J_2 = \int_0^{t_f} \left(\frac{2^R - 1}{K} s(x_1) + k_1 u^2 + k_2 x_2^2 + k_3 x_2 + k_4 \right. \\ & \left. + k_5 u + k_6 u x_2 \right) dt + C_1 ||x_1(t_f) - b||^2 \\ & + C_2 ||x_2(t_f) - d||^2 + C_3 ||x_3(t_f) - c||^2 \\ \text{subject to} \quad & \dot{x}_1(t) = x_2(t), \qquad x_1(0) = a, \\ & \dot{x}_2(t) = u(t), \qquad x_2(0) = 0, \\ & \dot{x}_3(t) = R(t), \qquad x_3(0) = 0, \\ & -u_{\max} \le u(t) \le u_{\max}, \quad 0 \le R(t) \le R_{\max}. \end{aligned} \tag{8}$$

While this simplifies the algorithm, it behooves us to ensure that the computed optimal control has its final state $x(t_f)$ be close enough to its specifications defined in (6) and (7) by appropriate selection of constants C_1, C_2 and C_3.

III. Algorithmic Approach

Consider the abstract optimal control problem whose state equation is

$$\dot{x} = f(x, u), \qquad x_0 := x(0) \ \text{ is given}, \tag{9}$$

where $x \in \mathscr{R}^n$ and $u \in \mathscr{R}^k$; the scalar-valued cost functional to be minimized is

$$J = \int_0^{t_f} L(x, u) dt; \tag{10}$$

and the input $u(t)$ has pointwise constraints of the form $u(t) \in U$ for a compact set $U \subset \mathscr{R}^k$. Suppose that the functions $f : \mathscr{R}^n \times \mathscr{R}^k \to \mathscr{R}^n$ and $L : \mathscr{R}^n \times \mathscr{R}^k \to \mathscr{R}$ are piecewise-continuously differentiable and locally Lipschitz continuous, and the final time t_f is given and fixed. Let $p(t) \in \mathscr{R}^n$ denote the costate (adjoint) equation, and recall that the Hamiltonian is defined via the following equation:

$$H(x, u, p) = p^{\mathrm{T}} f(x, u) + L(x, u), \tag{11}$$

whose Right-Hand Side's dependence on t is suppressed in the notation used.

Suppose that for every $x \in \mathscr{R}^n$ the function $f(x, u)$ is linear in u and the function $L(x, u)$ is convex in u; note that this does not mean that f is linear or L is convex jointly in both variables (x, u). Now let $u(t)$, $t \in [0, t_f]$, be an admissible control, namely a Lebesgue-measurable, absolutely integrable function from $[0, t_f]$ into U. Let $x(t)$ and $p(t)$ be the corresponding state trajectory and costate trajectory. Consider the Hamiltonian $H(x(t), u(t), p(t))$ as a function of $u(t) \in U$. Notice that $x(t)$ and $p(t)$ were derived from $u(t)$. For every

$t \in [0,t_f]$, let $u^\star(t) \in \arg\min(H(x(t),w,p(t))|w \in U)$ which we call a (pointwise) *minimizer of the Hamiltonian*. Observe that it need not be unique. Suppose that there exists an admissible control $u^\star(t)$ such that at every time $t \in [0,t_f]$, $u^\star(t)$ is a minimizer of the Hamiltonian in this fashion. The algorithm we next describe is suitable for problems where it is easy to compute the pointwise minimizer of the Hamiltonian.

Let $u(t)$ be a given admissible control, let $u^\star(t)$ be a minimizer of the Hamiltonian at each $t \in [0,t_f]$, and consider the control $u_{\text{next}}(t)$ defined in the following way.

1) Compute $\theta(u)$ defined as

$$\theta(u) = \int_0^{t_f} \big(H(x,u^\star,p) - H(x,u,p)\big)dt. \tag{12}$$

2) Compute the non-negative integer $k(u)$ defined as

$$k(u) := \min\big(k = 0,1,2,\ldots : J(u+2^{-k}(u^\star-u)) - J(u) \le 2^{-(k+1)}\theta(u)\big), \tag{13}$$

and define $\lambda(u) = 2^{-k(u)}$.

3) Set $u_{\text{next}} = u + \lambda(u)(u^\star - u)$.

The algorithm then repeats steps 1-3 until it converges.

Observe that this algorithm searches for u_{next} in the direction of $u^\star$ from u, and it is not a gradient descent but a sort of gradient projection. The stepsize yielding $u^\star$ in that direction is due to Armijo, and it is known to provide effective convergence to local minima, when used in conjunction with gradient-descent algorithms in the setting of nonlinear programming (see, e.g., [21] and references therein). In particular, these algorithms typically move quickly towards optimum points at the initial phases of their runs.

In the context of our energy-aware problem defined in (8), recall that the state variable is $(x_1(t),x_2(t),x_3(t))$ and the input is $(u(t),R(t))$, and let $p(t) = (p_1(t),p_2(t),p_3(t))$ be an explicit coordinate representation of the costate. By the costate equation, they have the forms

$$\begin{aligned} \dot{p}_1 &= -\frac{2^R-1}{K}\frac{\partial s(x_1)}{\partial x_1}, & p_1(t_f) &= 2C_1(x_1(t_f)-b),\\ \dot{p}_2 &= -p_1 - 2k_2x_2 - k_3 - k_6u, & p_2(t_f) &= 2C_2(x_2(t_f)-d),\\ \dot{p}_3 &= 0, & p_3(t_f) &= 2C_3(x_3(t_f)-c), \end{aligned} \tag{14}$$

and by (11), the Hamiltonian is given by

$$\begin{aligned} H(x,u,p) = p_1x_2 + p_2u + p_3R + \frac{2^R-1}{K}s(x_1) + k_1u^2 \\ + k_2x_2^2 + k_3x_2 + k_4 + k_5u + k_6ux_2, \end{aligned} \tag{15}$$

where the dependence on t is suppressed in the notation. It is readily seen that the minimizer of the Hamiltonian is given by

$$u^\star = \begin{cases} -\frac{(p_2+k_5+k_6x_2)}{2k_1} & \text{if } \left|\frac{(p_2+k_5+k_6x_2)}{2k_1}\right| \le u_{\max},\\ u_{\max} & \text{if } -\frac{(p_2+k_5+k_6x_2)}{2k_1} > u_{\max},\\ -u_{\max} & \text{if } -\frac{(p_2+k_5+k_6x_2)}{2k_1} < -u_{\max}, \end{cases}$$

and

$$R^\star = \begin{cases} \frac{1}{\ln(2)}\ln\left(\frac{-p_3K}{\ln(2)s(x_1)}\right) & \text{if } p_3 \le -\frac{(\ln(2)s(x_1))}{K},\\ R_{\max} & \text{if } \frac{1}{\ln(2)}\ln\left(\frac{-p_3K}{\ln(2)s(x_1)}\right) > R_{\max},\\ 0 & \text{otherwise.} \end{cases}$$

We observe that $R^\star$ is lower at points where $s(x_1)$ is higher and vice versa. This means that the robot should transmit at higher (lower) rates in places where the channel quality is higher (lower), as expected.

All but the terms $s(x_1) = E\left[\frac{1}{\gamma(q(x_1))}\right]$ and its derivative $\frac{\partial s(x_1)}{\partial x_1}$ in the RHS of (14) and (15) are explicit and can be easily calculated. $s(x_1)$ and its derivate can then be calculated by utilizing (4).

IV. Simulation Results

We coded our algorithm in MATLAB and ran it on a laptop with Intel dual core i5 3317U 1.7 GHz processor and 4GB 1600 MHz RAM. The problem we considered has the following parameters. The robot travels in a straight line with length of 25 meters in 20 seconds, and hence $t_f = 20$, $x_1(0) = 0$ and $x_1(t_f) = 25$. It moves towards the transmitter located 40 m from its initial placement, i.e. $q_b = 40$. The robot experiences the CNR of Fig. 1 across its path, which is based on real channel measurements (see [8] for details on the measurement setup). The channel is mainly unknown to the robot and is predicted based on 20% a priori measurements in the same environment by using the channel prediction framework of [7], [8], summarized in Section II-A. This results in the following channel parameters: $\alpha = -41.34$, $n_{\text{PL}} = 3.86$, $\xi_{\text{dB}} = 3.20$, $\beta = 3.09$ meters, and $\rho_{\text{dB}} = 2.77$. We used these to compute offline $s(x_1(t))$ and its derivative. We set the total number of information bits to be $Q/B = 100$ bits/Hz (i.e. $x_3(t_f) = 100$), and $R_{\max} = 6$ bits/Hz/s.

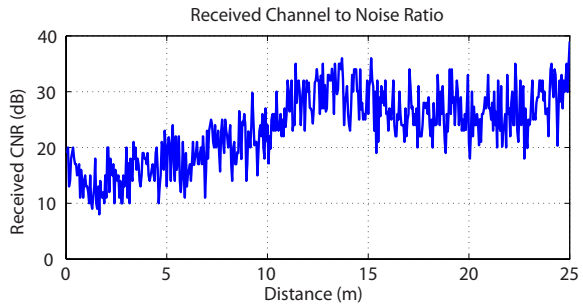

Fig. 1. The figure shows the CNR (based on real measurements) along a straight line with the length of 25 meters.

The motion cost parameters in (5) are set to $k_1 = 5.47$, $k_2 = 0.77$, $k_3 = 10.10$, $k_4 = 4.24$, $k_5 = 0$ and $k_6 = 0$ as in [13][2]. The upper bound on the acceleration is taken as $u_{\max} = 1\,\text{m/s}^2$. Moreover, the initial conditions in (8) are chosen as $x_2(0) = x_3(0) = 0$, the terminal velocity is chosen as $x_2(t_f) =$

[2]Note that we can consider $k_5 = 0$ and $k_6 = 0$ if the initial and final velocities of the robot are the same [13].

0, and the penalty weights of J_2 are $C_1 = 10$, $C_2 = 10$ and $C_3 = 10$.

The algorithm was run for 500 iterations, and the results are shown in Figures 2-6. All differential equations were solved via the forward Euler method based on the time-difference $\Delta t = 0.001$s. Fig. 2 plots the graph of the cost J_2 as a function of iteration count. It shows that much of the cost reduction occurs in about 20 iterations. Such rapid descent in the early stages of an algorithm's run are characteristic in gradient-descent algorithms with Armijo step sizes [21], and is one of the reasons we chose it as part of our computational technique. As a matter of fact, the initial cost is $J_2 = 1.0633 \times 10^5$ and after 20 iterations the cost is $J_2 = 540.54$. The cost at the end of 500 iterations is $J_2 = 402.47$. To gain a clearer view of the cost-descent, we plot the graph of J_2 from iteration 20 onwards in Fig. 3.

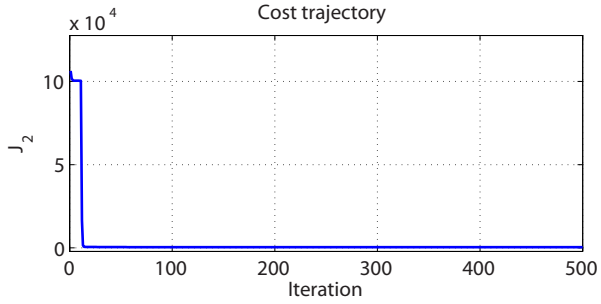

Fig. 2. The plot shows the anticipated total energy cost (J_2) as a function of iteration step. The cost almost reduces to its final value in about 20 iterations.

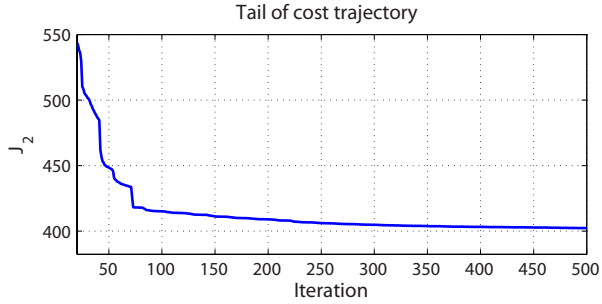

Fig. 3. The plot shows the tail of the curve in Fig. 2. The cost remains almost constant after the first few iterations.

The term $\theta(u)$ in (12) acts as an *optimality function*, namely a measure of the extent to which u fails to be an optimal control (see [21] for an extensive discussion on optimality functions and their role in optimization). To see this, observe that $\theta(u)$ is always non-positive since $u^\star$ minimizes the Hamiltonian. The condition $\theta(u) = 0$ is equivalent to the maximum principle, and $|\theta(u)|$ can be viewed as a measure of u failing to satisfy the maximum principle. Generally, a characterization of an algorithm's convergence can be based on how close $|\theta(u)|$ gets to zero (see [21]). As for our algorithm, Fig. 4, showing $\theta(u)$ as a function of iteration counts, indicates together with the tail of the graph in Fig. 3 that the algorithm has converged. We also mention that the final-state constraints of $x_1(t_f) = 25$, $x_2(t_f) = 0$ and $x_3(t_f) = 100$ are almost met, with the obtained values of $x_1(t_f) = 24.42$, $x_2(t_f) = 0.21$ and $x_3(t_f) = 99.91$. Choosing larger values of C_1, C_2 and C_3 only makes the asymptotic convergence slower without any significant gains on the accuracy of final states, which are already very close to the desired values for the given choices of C_1, C_2 and C_3.

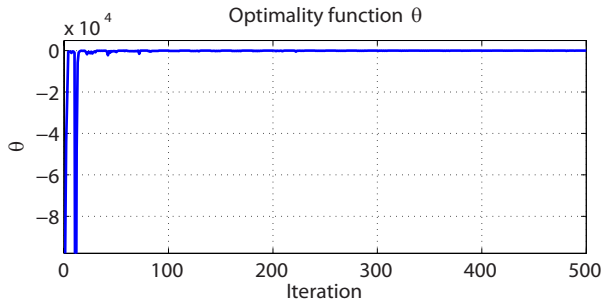

Fig. 4. Optimality function quickly goes to zero as algorithm converges.

Remark. Due to the disparate nature of our control variables u and R we use block iterations in the algorithm, namely, we cycle between 10 iterations in u for a fixed R and then 10 iterations in R for a fixed u. The effect of this can be seen for example in Fig. 3, where the cost-reduction is more pronounced at the start of a block than at its end.

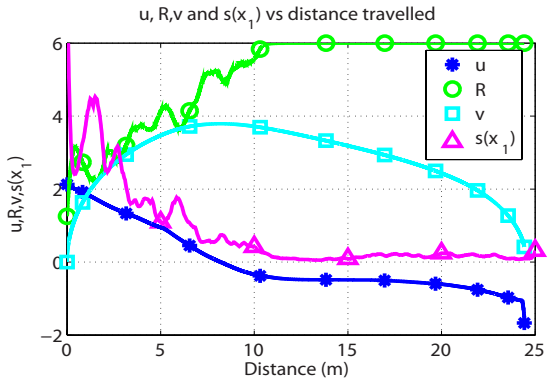

Fig. 5. The acceleration u, spectral efficiency R, velocity $v = x_2$ and channel $s(x_1)$ along the path of travel. u and v are magnified by factor 5 and 2 respectively while $x_1(t)$ and $s(x_1)$ are scaled by factor of 8 and 2 respectively. We can clearly see how the robot adapts its communication and motion strategies based on the predicted channel quality metric ($s(x_1)$). The delay caused by the acceleration cost can also been observed.

Fig. 5 depicts the computed optimal controls and robot behaviors at different points along the path while Fig. 6 shows their evolution in time domain. It can be seen that periods of higher predicted channel quality (low $(s(x_1))$) correspond to larger spectral efficiency (R) as one would have expected. Moreover, the spectral efficiency changes instantaneously to changes in channel quality. The velocity response is a bit delayed to changes in channel quality and is quite smooth. This can be ascribed to using acceleration as an input and defining a cost on velocity. Again, the acceleration profile is very smooth due a cost defined on it. This behavior stands in contrast to the findings of [19] which, using the velocity as a control in a (discrete-time) co-optimization problem,

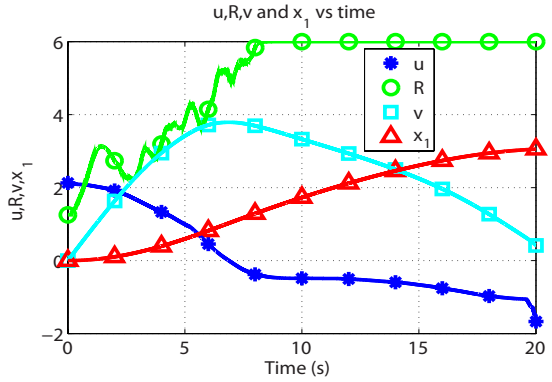

Fig. 6. The acceleration u, spectral efficiency R, velocity $v = x_2$ and distance traveled x_1 vs time. u and v are magnified by factor 5 and 2 respectively while $x_1(t)$ is scaled by factor 8. We can clearly see how the robot adapts its communication and motion strategies based on the predicted channel quality metric ($s(x_1)$). The delay caused by the acceleration cost can also been observed.

Δt	iterations	Final Cost	CPU Time	Final Position	Final Velocity	Bits/Hertz
0.001	500	402.40	56.23	24.42	0.21	99.91
0.001	250	406.20	28.03	24.43	0.40	99.90
0.005	500	402.50	12.35	24.44	0.20	99.89
0.005	250	405.50	6.18	24.44	0.33	99.88
0.010	500	403.50	7.10	24.42	0.25	99.90
0.010	250	406.70	3.49	24.43	0.40	99.86
Initial Cost = 1.0633e5; CPU time in seconds						

TABLE I

TABLE SHOWS THE RESULTS OF SIMULATIONS FOR VARIOUS STEPS SIZES AND NUMBER OF ITERATIONS.

yields wider variations in velocity $v(t)$, and hence large accelerations $|u(t)|$. In practical situations, the acceleration may be limited due to operational constraints and hence its explicit inclusion in the optimal control problem appears to be a more practical approach. To bring the final velocity to zero, we see a sharp deceleration towards the end.

To test the efficiency of our approach, we ran the algorithm for different time steps used in the numerical integration, as well as different numbers of iterations. The results for $\Delta t = 0.001, 0.005, 0.01$ seconds, and for 250 and 500 iterations, are shown in Table I. While we observe significant changes in the CPU times of the three runs, we note that the final results of the computations are quite close to each other. In particular for $\Delta t = 0.01$ s and 250 iterations, the algorithm's run was completed in 3.49 seconds on CPU time. This indicates the potential use of our algorithm for real time applications.

V. Conclusions

In this paper, we considered a scenario where a mobile robot needs to transmit a fixed number of information bits to a remote station in a realistic fading environment, while moving along a fixed trajectory. Our goal is to minimize the total energy cost, including both communication and motion energy consumption, while satisfying time budget and communication reception constraints. We considered a second-order dynamic model for the motion of the robot and adopted a more general motion cost model which incorporates the impact of acceleration. We posed the problem in an optimal control framework in the continuous time domain to make it amenable to maximum principle and hence our efficient Hamiltonian-based algorithm. We demonstrated how the robot adapts its communication and motion strategies accordingly based on the predicted channel quality. In particular, our results indicated the delayed response of the velocity of the robot to the predicted channel quality due to the presence of acceleration in motion dynamics and cost. The strengths of our algorithm were demonstrated by showing its property of fast convergence to the optimal solution and its fast execution times.

References

[1] F. Bullo, E. Frazzoli, M. Pavone, K. Savla, and S. L. Smith, "Dynamic vehicle routing for robotic systems," *Proceedings of the IEEE*, vol. 99, no. 9, pp. 1482–1504, September 2011.

[2] M. M. Zavlanos, M. B. Egerstedt, Y. C. Hu, and G. J. Pappas, "Graph-theoretic connectivity control of mobile robot networks," *Proceedings of the IEEE*, vol. 99, no. 9, pp. 1525 – 1540, July 2011.

[3] S. L. Smith, M. Schwager, and D. Rus, "Persistent robotic tasks: Monitoring and sweeping in changing environments," *IEEE Transaction on Robotics*, vol. 28, no. 2, pp. 410–426, April 2012.

[4] A. Ghaffarkhah and Y. Mostofi, "Communication-aware motion planning in mobile networks," *IEEE Transactions on Automatic Control, special issue on Wireless Sensor and Actuator Networks*, vol. 56, no. 10, pp. 2478–2485, 2011.

[5] Y. Yan and Y. Mostofi, "Robotic router formation in realistic communication environments," *IEEE Transactions on Robotics*, vol. 28, no. 4, pp. 810 – 827, August 2012.

[6] ——, "To go or not to go: On energy-aware and communication-aware robotic operation," *IEEE Transactions on Control of Network Systems*, vol. 1, no. 3, Sept. 2014.

[7] Y. Mostofi, M. Malmirchegini, and A. Ghaffarkhah, "Estimation of communication signal strength in robotic networks," in *Proc. of IEEE Int'l Conf. on Robotics and Automation*, May 2010, pp. 1946–1951.

[8] M. Malmirchegini and Y. Mostofi, "On the spatial predictability of communication channels," *IEEE Trans. on Wireless Comm.*, vol. 11, no. 3, pp. 964–978, Mar. 2012.

[9] N. Wagle and E. Frew, "Transfer learning for dynamic rf environments," in *American Control Conference (ACC)*, 2012, pp. 1406–1411.

[10] J. Fink, A. Ribeiro, and V. Kumar, "Robust control for mobility and wireless communication in cyber–physical systems with application to robot teams," *Proc. of the IEEE*, vol. 100, no. 1, pp. 164–178, 2012.

[11] A. Kopeikin, S. Ponda, L. Johnson, and J. How, "Multi-uav network control through dynamic task allocation: Ensuring data-rate and bit-error-rate support," in *IEEE Globecom Workshop on Wireless Networking for Unmanned Autonomous Vehicles*, 2012, pp. 1579–1584.

[12] A. Goldsmith, *Wireless Comm.* Cambridge Univ. Press, 2005.

[13] P. Tokekar, N. Karnad, and V. Isler, "Energy-optimal trajectory planning for car-like robots," *Autonomous Robots*, pp. 1–22, 2013.

[14] Y. Mei, Y.-H. Lu, Y. C. Hu, and C. S. G. Lee, "Deployment of mobile robots with energy and timing constraints," *IEEE Transaction on Robotics*, vol. 22, no. 3, pp. 507–522, June 2006.

[15] C. C. Ooi and C. Schindelhauer, "Minimal energy path planning for wireless robots," *Mobile Networks and Applications*, vol. 14, no. 3, pp. 309–321, January 2009.

[16] F. El-Moukaddem, E. Torng, G. Xing, and G. Xing, "Mobile relay configuration in data-intensive wireless sensor networks," *IEEE Transactions on Mobile Computing*, vol. 12, no. 2, pp. 261–273, 2013.

[17] C. Tang and P. McKinley, "Energy optimization under informed mobility," *IEEE Transactions on Parallel and Distributed Systems*, vol. 17, no. 9, pp. 947–962, 2006.

[18] H. Jaleel, Y. Wardi, and M. Egerstedt, "Minimizing mobility and communication energy in robotic networks: An optimal control approach," in *IEEE American Control Conference*, 2014, pp. 2662 – 2667.

[19] Y. Yan and Y. Mostofi, "Co-optimization of communication and motion planning of a robotic operation under resource constraints and in fading environments," *Wireless Communications, IEEE Transactions on*, vol. 12, no. 4, pp. 1562–1572, 2013.

[20] H. J. M. Hale, Y. Wardi and M. Egerstedt, "Hamiltonian-based algorithm for optimal control of switched-mode hybrid systems," in *Technical Memorandum*, Georgia Tech, 2014.

[21] E. Polak, *Optimization: algorithms and consistent approximations*. Springer-Verlag New York, Inc., 1997.